

A HIGH CURRENT INJECTOR FOR THE PROPOSED SLAC LINEAR COLLIDER*

M. B. James and R. H. Miller
 Stanford Linear Accelerator Center
 Stanford University, Stanford, California 94305

Abstract

A new, high-current injector has been designed to yield the $7.5 \times 10^{10} e^-$ per S-band bunch necessary for the proposed linear collider.¹ The injector consists of two prebunchers at the 16th subharmonic, a 0.75 c traveling wave buncher, and a three-meter velocity of light traveling wave structure. The e^- beam is confined by a solenoidal magnetic field in the buncher and capture regions. A computer simulation similar to that used by Mavrogenes et al.,² has been used to calculate the bunching. The calculation indicates it is possible to achieve $\sim 1 \times 10^{11} e^-$ in 16° of S-band from a 15 amp gun pulse of 1.5 nsec duration.³

Requirements of the SLC High-Current Injector

The SLC injector must produce two, single-bunch electron pulses approximately 60 nsec apart. The leading bunch is used for electron/positron collisions in the collider interaction region, while the trailing bunch is used to produce positrons at the two-thirds point of the existing linac. Each bunch must contain at least 7.5×10^{10} electrons in a single S-band wavelength. The emittance must not be greater than $3 \times 10^{-2} \text{ mm}_0\text{-cm}$.

General Description of the SLC Injector

The SLC injector (Fig. 1) consists of a 200 kV electron gun, a prebuncher at the 16 subharmonic followed by a 108 cm drift space, a second 16th subharmonic buncher followed by a 36 cm drift space, a traveling wave buncher, a three-meter velocity of light traveling wave section and a two-meter drift section for beam measurement instrumentation. The electron beam is confined by a solenoidal magnetic field in the buncher and capture regions which radially focuses the beam. Each component of the injector is described below.

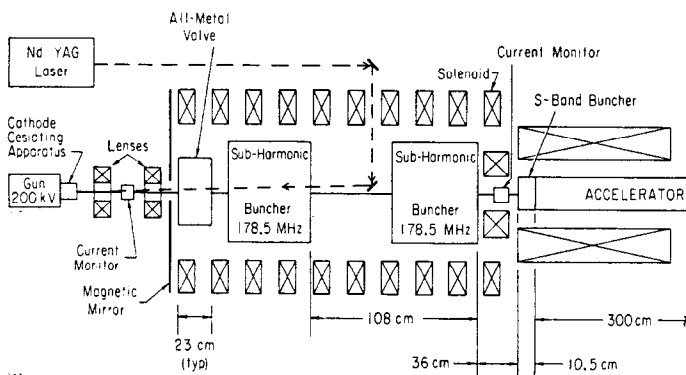


Fig. 1. The SLC injector.

Electron Gun. Two different electron guns have been designed and built for the SLC injector. The first source uses a Nd:YAG laser to produce electrons by photoemission from a semiconductor cathode.³ The second source is a conventional thermionic emission source.⁴ Each source should produce a 15 amp, roughly Gaussian-shaped pulse with $\sigma \approx 0.5$ nsec.

Subharmonic Buncher Cavities. The subharmonic bunchers are one-fourth wavelength, coaxial, copper cavities,⁵ whose inner conductors have a 4 cm gap at one end. The cavities have Q_0 equal to 12,000 and a shunt impedance of 2.2 M Ω . Since it is important that the two electron bunches, 60 nsec apart, see the same electric field across the gap, we have over-coupled the cavity so that $Q_L = 4000$ which shortens the rise time of the pulse appropriately. The subharmonic buncher frequency was chosen low enough so that the 1.5 nsec gun pulse falls within the substantially linear region of the sinusoidal electric field. A lower frequency would work as well, but would require higher peak fields. In the drift regions following the subharmonic bunchers we have made the diameters of the surrounding conducting cylinders as small as possible. Our computer calculations have shown that the image charges in the conducting cylinder significantly reduce the space charge effects and, hence, improve bunching.

Buncher and Accelerator Regions. The 10.5 cm long traveling wave buncher with constant phase velocity of 0.75 C and the three-meter velocity of light traveling wave accelerator sections are identical to those used in the existing SLAC linac.⁶ These sections will bunch electrons which are within $\pm 90^\circ$ S-band into a small bunch on the crest of the accelerator RF.

Magnetic Focusing. The beam from the gun is focused by two magnetic thin lenses so that we can adjust the radius and convergence of the beam at the entrance to solenoid which confines the beam in the subharmonic buncher region. The nominal design produces a waist with a 1 cm radius at this point. The field in the subharmonic buncher solenoid tapers from 150 gauss at the input to 500 gauss at the output to keep the beam radius constant as the charge density increases due to bunching. At this point the field is raised to focus the beam down to a 5 mm radius in the S-band buncher and the capture region of the accelerator section. In this region the focusing field rises from about 1 kg to a maximum of about 2 kg, and then decreases as the beam gains energy.

Calculation of Bunching

For purposes of calculation, we have assumed that the initial pulse from either the laser or thermionic gun can be approximated as a 15 amp peak Gaussian shaped beam with $\sigma = 0.48$ nsec. We modeled the beam as 51 infinitely thin disks of charge with each disk divided into three concentric annular regions of equal charge. The program calculates the longitudinal position and energy of the annular regions as they move through the injector region. The space charge forces between the annuli are found by solving for the average static force between annuli surrounded by a grounded conducting cylinder. Thus the program calculates the effects of space charge and image charges. Briefly, the calculation is as follows:^{2,7} the potential of a point charge located at $r = b$, $\theta = \phi$ in an infinite conducting cylinder of radius a is:

$$\psi_{pt}(r, \theta, z) = \frac{\rho}{\pi \epsilon_0 a} \sum_{m=0}^{\infty} \sum_{n=1}^{\infty} \left\{ \frac{1}{1 + \delta_{mo}} \left[\frac{J_m \left(\frac{j_{mn} b}{a} \right) J_m \left(\frac{j_{mn} r}{a} \right)}{\left(j_{mn} J_{m+1} \left(j_{mn} \right) \right)^2} \right] \times \left(e^{-(j_{mn}/a)|z|} \right) \cos(\theta - \phi) \right\} \quad (1)$$

where

* Work supported by the Department of Energy, contract DE-AC03-76SF00515.

J_m = the mth Bessel function.

j_{mn} = nth zero of the mth Bessel function.

ρ = charge density

The potential of an annulus of charge with inner radius b_1 and outer radius b_2 is

$$\psi(r, \theta, z) = \int_{b_1}^{b_2} \int_0^{2\pi} \psi_{pt}(r, \theta, z; b, \phi) b db d\phi \quad (2)$$

The longitudinal electric field is found by differentiating the potential.

$$E_z(r, \theta, z) = -\frac{\partial \psi}{\partial z} = -\frac{\partial}{\partial z} \int_{b_1}^{b_2} \int_0^{2\pi} \psi_{pt}(r, \theta, z; b, \phi) b db d\phi \quad (3)$$

Given a second annulus of charge located at z , with inner radius r_1 , and outer radius r_2 , the average longitudinal field on the second ring due to the first ring is

$$\bar{E}_{21} = \frac{\int_{r_1}^{r_2} \int_0^{2\pi} E_z(r, \theta, z) r dr d\theta}{\int_{r_1}^{r_2} \int_0^{2\pi} r dr d\theta} \quad (4)$$

$$= \int_{r_1}^{r_2} \int_0^{2\pi} \int_{b_1}^{b_2} \left\{ -\frac{\partial}{\partial z} \psi_{pt}(r, \theta, z; b, \phi) \right\} b db d\phi r dr d\theta / \pi(r_2^2 - r_1^2).$$

The change in the energy of the second disk due to this average field is

$$\frac{dY_2}{dz} = \frac{e}{m_0 c^2} \bar{E}_{21} \quad (5)$$

where

e = charge of electron
 m_0 = mass of electron
 c = speed of light in vacuum .

The variable z in the exponent of Eq. (1) represents the distance between the two rings. If we measure the position of each disk by its phase relative to a wave with $\lambda f = c$, the approximate distance between the rings in the lab frame is

$$z \approx \frac{v_1}{c} \lambda \frac{\theta_2 - \theta_1}{2\pi} \quad (6)$$

where

θ_1 = phase of annulus 1
 θ_2 = phase of annulus 2
 v_1 = velocity of annulus 1 .

Since we are calculating the force on the second ring, we must write this distance in the second ring's frame

$$z = \gamma_2 \beta_1 \frac{\theta_2 - \theta_1}{2\pi} \lambda \quad (7)$$

This relativistic correction differs from that used by Mavrogenes.⁴ However, we believe it to be a better approximation since it reduces the correct answer, $E = \rho/2\epsilon_0$, at $z=0$. Performing the integration in Eq. (4) and summing over all 50 rings, we find the change in energy of a given annulus m due to all other annuli is

$$\frac{dY_m}{dz} = \frac{2e}{\epsilon_0 m_0 c^2} \frac{Q}{\pi(r_{m2}^2 - r_{m1}^2)} \quad (8)$$

$$\times \sum_{n=1}^{\infty} \sum_{\substack{j=1 \\ j \neq m}}^{NA} e^{-t_j^2/2\sigma^2} \frac{r_{m2} J_1(j_{on} \frac{r_{m2}}{a}) - r_{m1} J_1(j_{on} \frac{r_{m1}}{a})}{(r_{j2}^2 - r_{j1}^2)}$$

$$\times \frac{r_{j2} J_1(j_{on} \frac{r_{j2}}{a}) - r_{j1} J_1(j_{on} \frac{r_{j1}}{a})}{[j_{on} J_1(j_{on})]^2} e^{-\left| \frac{j_{on}}{a} \gamma_m \beta_j (\theta_m - \theta_j) \right|}$$

where

n = index for sum over the zeros of J_0

j = index for sum over all other rings

NA = number of annuli

$Qe^{-t_j^2/2\sigma^2}$ = the total charge on each annular region

t_j = time the j th annulus leave the gun

σ = sigma of longitudinal Gaussian charge distribution

r_{j1} = inner radius of j th ring

r_{j2} = outer radius of j th ring

The change in the position of the annulus relative to a wave with phase velocity β_p and wavelength λ is

$$\frac{d\theta_m}{dz} = \frac{2\pi}{\lambda} \left(\frac{1}{\beta_p} - \frac{1}{\beta_m} \right) \quad (9)$$

Equations (8) and (9) were used to find the effects of space charge on each annular region due to all other annuli. The force due to the RF was modeled as a sinusoidal field at the fundamental frequency in each region:

$$\frac{dY_m}{dz} \Big|_{RF} = \frac{eE}{m_0 c^2} \sin \theta_m \quad (10)$$

where

E = electric field due to RF .

This model is best suited to the subharmonic buncher region where the conducting cylinders are smooth. In the buncher and accelerator regions made up of disk loaded waveguides, this model is a great oversimplification.

Results of Calculations

The results of the calculations are shown in Figs. 2(a) and 2(b). In each case we plot initial phase vs final phase for four locations: the end of the drift spaces following the two subharmonic bunchers, the end of the 10.5 cm buncher and the end of the three-meter accelerator section. We began by assuming we would need only one subharmonic buncher. By varying the SHB voltage and the length of the drift section, we hoped to bunch sufficiently to obtain a single bunch in the S-band buncher. We found that bunching was badly asymmetric as the front of the pulse was quite overbunched by the time the back of the pulse was adequately bunched. Varying the voltage and length of the drift space did not alleviate this problem. Therefore, after a one-meter drift we added a second subharmonic buncher which accelerates the back of the pulse and improves the bunching significantly. With this configuration we calculated that we would bunch 8.1×10^{10} electron in 14° of S-band. Figure 2(b) is included to show the effect of a larger pipe radius on bunching. The small diameter pipe used in the subharmonic buncher regions reduces the space charge forces since the electric field of each annulus falls off faster than $e^{-2.4z/a}$ where a is the radius of the pipe. The field falls to 1% of its peak value when $z/a = 2$. It is evident to us that the answers obtained depend somewhat on the number of annular regions we choose. Since increasing the number of annuli also increases computing time, we plan to improve the model by smoothing the forces between annuli at short-distances.

Emittance

A dominant feature of the optics of the SLC injector is the radial force produced by the RF fields in the subharmonic bunchers, the S-band buncher and the capture region of the accelerator section. To a good approximation they vary linearly with radius and, of course,

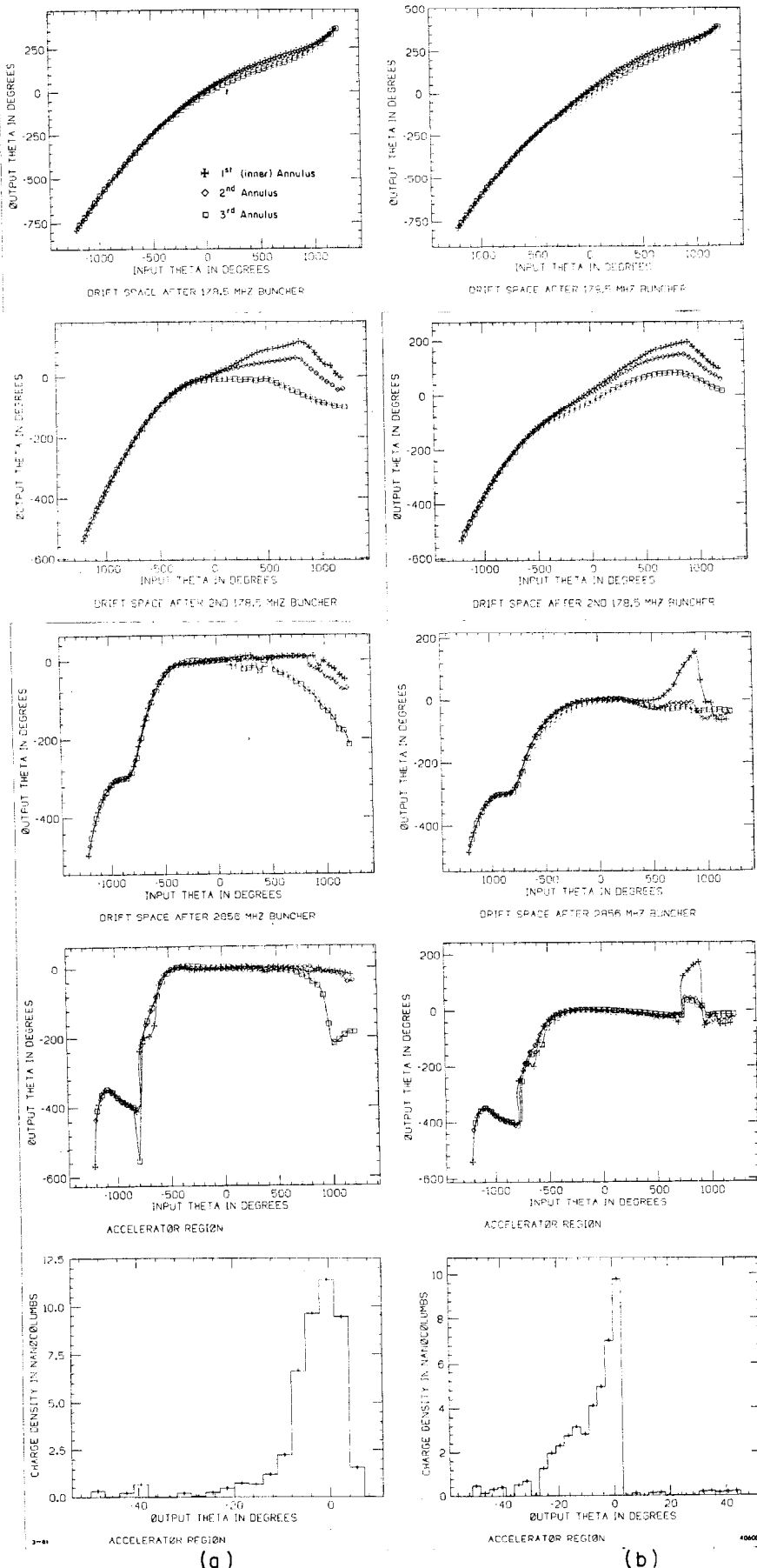


Fig. 2. Results of the buncher calculations: (a) with 3.5 cm beam pipe in subharmonic buncher region, final bunch, $\sigma = 7^\circ$ with 8×10^{10} electrons within $\pm\sigma$. (b) 10 cm beam pipe, $\sigma = 12^\circ$.

sinusoidally with time with the frequency of RF in each device. Thus each of these devices is a time varying lens. The maximum divergent strength of these lenses occur at the longitudinal electric field null around which the electrons bunch. The significant problem is not that these lenses are divergent for the electrons which form the bunch, but rather that they are time-varying. Thus, the electrons passing through each region are focused differently as a function of time and their projection into a single transverse phase plane increases in area.

The emittance introduced by the subharmonic buncher is

$$\mathcal{E}_{shb} = 1.5 \times 10^{-3} \pi m_0 c/cm$$

for a 1 cm radius beam entering over a phase interval of $\pm 30^\circ$ (at 178.5 MHz).

The S-band buncher is much worse because of the shorter wavelength. For a beam radius of 0.5 cm and a phase interval of $\pm 80^\circ$ (at 2856 MHz) the increase in emittance is

$$\mathcal{E}_{gun} = 1.0 \times 10^{-2} \pi m_0 c/cm$$

Finally, the electrons enter the accelerator capture region with an energy of 250 keV, a beam radius of 0.5 cm and a phase interval of $\pm 15^\circ$. The emittance increase is

$$\mathcal{E}_{acc} = 1.7 \times 10^{-2} \pi m_0 c/cm$$

Reducing the beam radius would reduce these emittance growths but would degrade the longitudinal bunching. In the subharmonic buncher region where the transverse emittance growth is negligible (and localized) the beam will be as large as possible consistent with good transmission.

Acknowledgements

We wish to thank J. C. Sheppard and S. J. Hutton for their valuable contributions to the computer calculations. We also wish to thank K. L. Porzuczek, D. A. Nevius, B. A. Laurie and H. Fischer for their contributions to the mechanical design and installation of the SLC injector.

References

1. SLAC Linear Collider Conceptual Design Report, SLAC Report No. 229, June 1980.
2. G. Mavrogenes *et al.*, IEEE Trans. Nucl. Sci. **NS-20**, 919, June 1973.
3. C. Sinclair, Proceedings of the 1981 Particle Accelerator Conference, March 11-13, 1981.
4. R. Koontz *et al.*, Proceedings of the 1981 Particle Accelerator Conference, March 11-13, 1981.
5. Subharmonic Buncher Cavity Designed by W. J. Gallagher, Boller-Gallagher Engineering Co., Alameda, CA 94501.
6. R. H. Miller *et al.*, IEEE Trans. Nucl. Sci. **NS-12**, 804 (1965).
7. C. B. Williams and M. H. MacGregor, IEEE Trans. Nucl. Sci. **NS-14**, 581 (1967).